

MODE DOMAIN SPATIAL ACTIVE NOISE CONTROL USING SPARSE SIGNAL REPRESENTATION

Yu Maeno^{*}, Yuki Mitsufuji^{*}, and Thushara D. Abhayapala[†]

^{*}Sony Corporation, Minato-ku, Tokyo, Japan

[†]Research School of Engineering, The Australian National University, Canberra ACT 2601, Australia

ABSTRACT

Active noise control (ANC) over a sizeable space requires a large number of reference and error microphones to satisfy the spatial Nyquist sampling criterion, which limits the feasibility of practical realization of such systems. This paper proposes a mode-domain feedforward ANC method to attenuate the noise field over a large space while reducing the number of microphones required. We adopt a sparse reference signal representation to precisely calculate the reference mode coefficients. The proposed system consists of circular reference and error microphone arrays, which capture the reference noise signal and residual error signal, respectively, and a circular loudspeaker array to drive the anti-noise signal. Experimental results indicate that above the spatial Nyquist frequency, our proposed method can perform well compared to a conventional methods. Moreover, the proposed method can even reduce the number of reference microphones while achieving better noise attenuation.

Index Terms— Active noise control, adaptive algorithm, mode-domain signal processing, compressive sensing, sparse signal representation

1. INTRODUCTION

Spatial ANC systems aim to attenuate undesired noise over a spatial region by generating an anti-noise sound field over the region using secondary sources. Such a system is viewed as an extension to the well-studied single-channel ANC [1]–[3] to a multi-channel system [1], [4]. However, to control a sound field over an extended region needs a large number of reference and error microphones, to capture the reference noise signals and residual error signals, respectively, as well as many loudspeakers to generate the anti-noise. The requirement to have many microphones limits the viability of using spatial ANC systems in practice. Nevertheless, in most practical applications [5], [6], the underlying noise field is due to a small number of underlying noise sources. In this paper, we aim to reduce the number of microphones required by spatial ANC systems by using a sparse signal representation.

In practice, multiple-channel ANC in the frequency domain [7], [8] is widely used to attenuate the noise field at multiple points where the error microphones are placed. One drawback of this approach to create a large quiet zone is the requirement to uniformly place many error microphones inside the control region. In contrast, spatial-sound-field representation techniques, such as wave field synthesis (WFS) [9] and higher order ambisonics (HOA) [10], [11] are promising techniques to control not only multiple points but the entire space of interest. These techniques have been applied to ANC and have shown that mode-domain ANC can achieve noise attenuation over a large space even with less computational complexity [12]–[14]. However, such systems still require a large number of microphones

and loudspeakers to reproduce the sound field properly, thus limiting the feasibility of practical implementations. Without a theoretically sufficient number of sensors, the system suffers from artifacts due to spatial aliasing [15] due to violating the spatial Nyquist sampling criterion.

One way to alleviate the aliasing restriction is by expressing the noise field using only a small number of basis functions from an over complete dictionary. This approach is well known as compressive sensing (CS) [16], which can provide an accurate solution for underdetermined problems where the sparse characteristic of the underlying signal field is usually used to solve the problem [17].

In this paper, we propose a mode-domain ANC system that can perform noise attenuation in large space beyond the spatial Nyquist frequency using few reference microphones than required by Nyquist theory. We represent the reference noise field as a superposition of weighted plane waves impinging from the far field. Using the estimated plane wave weights calculated by adopting several types of CS methods, we reconstruct the reference mode coefficients, which are expected to include less artifacts caused by spatial aliasing. The proposed methods are evaluated and compared in terms of reference-noise-field reproduction accuracy and noise attenuation level. We demonstrate that our proposed method can overcome the spatial Nyquist frequency limitation. Furthermore, we show that the number of reference microphones can be reduced while controlling the noise field properly.

Nicolas [18] proposed CS sound field reproduction based on plane wave decomposition by introducing a HOA-based constraint. However, they calculated the loudspeaker weights using amplitude-panning, which cannot be used directly for mode-domain processing. Jihui [19], [20] proposed the sparse complex FxLMS algorithm although they applied the CS approach to calculate sparse loudspeaker weights so that the spatial-aliasing artifacts cannot be avoided, which is caused by the spatial sampling of the microphone array.

2. PROBLEM STATEMENT

Let us consider a circular microphone array capturing a noise field generated by noise sources outside the microphone array in 2D space. We can represent an incident noise field at an arbitrary point $\mathbf{x} \equiv (r, \phi)$:

$$S(\mathbf{x}, k) = \sum_{m=-\infty}^{\infty} \beta_m(k) J_m(kr) e^{im\phi} \quad (1)$$

$$\approx \sum_{m=-M}^M \beta_m(k) J_m(kr) e^{im\phi}, \quad (2)$$

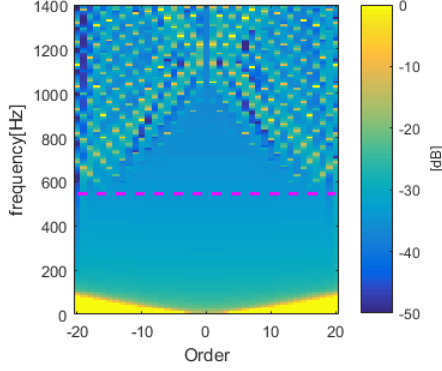


Fig. 1. Extracted circular mode coefficients of cylindrical wave using microphone outputs. The horizontal broken line indicates the spatial Nyquist frequency.

where $k = 2\pi f/c$ is the wave number, f is the frequency, c is the speed of sound, $\beta_m(k)$ is the m th-order circular mode coefficient, and $J_m(\cdot)$ is the m th-order Bessel function. In practice, (1) can be truncated to $M = \lceil ekR/2 \rceil$ [21] or $M = \lceil kR \rceil$ [22], where R is the radius of a controllable spatial region. The mode coefficient can be calculated utilizing orthogonal exponential functions:

$$\beta_m(k) = \frac{1}{QJ_m(kr)} \sum_{q=1}^Q S(\mathbf{x}, k) e^{-im\phi_q}, \quad (3)$$

where Q is the number of microphones and ϕ_q is the azimuth angle of the q th microphone. We need at least $Q \geq 2M+1$ microphones to avoid spatial aliasing [23]. Figure 1 shows the mode coefficients of the noise field captured by a 41-element circular microphone array of radius 2 m. The maximum order of the mode coefficients is $M = 20$. Observe that spatial aliasing artifacts appear for higher modes above 546 Hz, which is the spatial Nyquist frequency for this condition. The high amplitude of low frequency corresponds to an evanescent wave [24] of the cylindrical source. This evanescent component only exists near the source, and the amplitude decays exponentially [15]. Therefore, we assume that the impact on the performance of an ANC system inside the control region is minimal.

Our objective is to derive an algorithm to acquire precise reference mode coefficients of a noise field, which are then used to perform ANC instead of using direct mode coefficient extraction (3) containing spatial aliasing artifacts caused by the theoretical restriction, i.e. $M = \lceil kR \rceil$. We expect the noise field can be attenuated at higher frequencies beyond the spatial Nyquist frequency, even with an insufficient number of microphones.

3. PLANE WAVE WEIGHT ESTIMATION

In this section, we derive mode coefficient reconstruction based on plane wave decomposition assuming that the noise field is constructed by a superposition of weighted plane waves. The weights of the plane waves can be estimated accurately by utilizing the CS approach, which can be used to derive a sparse solution using only a few measurements.

As an alternative to (2), the noise field can be described by L plane waves impinging towards the coordinate origin [25]:

$$S(\mathbf{x}, k) = \sum_{\ell=1}^L \gamma_{\ell} e^{ik\hat{\mathbf{y}}_{\ell} \cdot \mathbf{x}}, \quad (4)$$

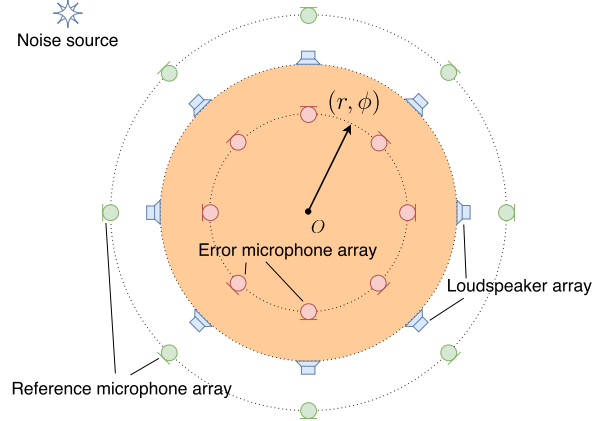


Fig. 2. Geometric setup of feedforward ANC system. The colored circle indicates the control region.

where γ_{ℓ} is the weight of ℓ th plane wave and $\hat{\mathbf{y}}_{\ell} \equiv (1, \phi_{\ell})$ is a unit vector towards the direction of the ℓ th plane wave. Circular expansion of the incident noise field due to an unit-magnitude plane wave is given by

$$e^{ik\hat{\mathbf{y}}_{\ell} \cdot \mathbf{x}} = \sum_{m=-M}^M i^m e^{-im\phi_{\ell}} J_m(kr) e^{im\phi}. \quad (5)$$

From (4) and (5), we have

$$S(\mathbf{x}, k) = \sum_{m=-M}^M i^m \underbrace{\sum_{\ell=1}^L \gamma_{\ell} e^{-im\phi_{\ell}}}_{\beta_m(k)} J_m(kr) e^{im\phi}. \quad (6)$$

Equation (6) shows that the mode coefficient $\beta_m(k)$ can be reconstructed using the plane wave weight γ_{ℓ} to reproduce the incident noise field.

In order to apply CS and estimate a sparse solution in (4), we represent it in matrix form:

$$\mathbf{s} = \mathbf{E}\boldsymbol{\gamma}, \quad (7)$$

where \mathbf{s} is a $Q \times 1$ vector of the observed signals, $\boldsymbol{\gamma}$ is an $L \times 1$ vector of plane wave weights, and \mathbf{E} is a $Q \times L$ matrix given by

$$\mathbf{E} = \begin{bmatrix} e^{ik\hat{\mathbf{y}}_1 \cdot \mathbf{x}_1} & \dots & e^{ik\hat{\mathbf{y}}_L \cdot \mathbf{x}_1} \\ \vdots & \ddots & \vdots \\ e^{ik\hat{\mathbf{y}}_1 \cdot \mathbf{x}_Q} & \dots & e^{ik\hat{\mathbf{y}}_L \cdot \mathbf{x}_Q} \end{bmatrix}. \quad (8)$$

We assume that the composition of plane waves is sparse with the underdetermined condition ($Q < L$) in (7).

3.1. ℓ_1 -norm constrained minimization

One of the most widely used technique to estimate a sparse solution is to minimize a cost function with an ℓ_1 constraint on the plane wave weights:

$$\mathcal{J} = \|\mathbf{v}\|_2^2 + \lambda_1 \|\boldsymbol{\gamma}\|_1, \quad (9)$$

where $\mathbf{v} = \mathbf{s} - \mathbf{E}\boldsymbol{\gamma}$ and λ_1 controls the strength of the sparsity constraint. By utilizing the steepest descent algorithm, we can update the weights $\boldsymbol{\gamma}$ as

$$\boldsymbol{\gamma}(n+1) = \boldsymbol{\gamma}(n) - \frac{\mu_{\text{mic}}}{2} \nabla \mathcal{J}(n), \quad (10)$$

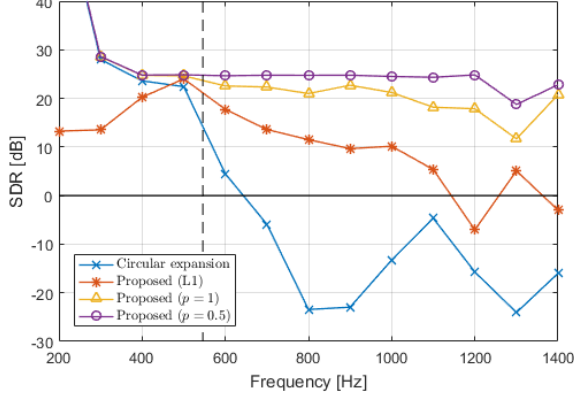


Fig. 3. SDR of reference sound field at several frequency bins. The vertical broken line indicates the spatial Nyquist frequency corresponding to the reference microphone array.

where n is the iteration index and μ_{mic} is the step size. A gradient of the cost function $\mathcal{J}(n)$ can be calculated as [19], [20]

$$\nabla \mathcal{J}(n) = 2\mathbf{E}^H \mathbf{v}(n) + \lambda_1 \left(\text{sgn}\{\Re\{\gamma(n)\}\} + i \text{sgn}\{\Im\{\gamma(n)\}\} \right), \quad (11)$$

where $(\cdot)^H$ denotes the Hermitian-transpose operation, $\text{sgn}(\cdot)$ denotes the sign function, and $\Re(\cdot)$ and $\Im(\cdot)$ denote the real and imaginary parts of the argument. Finally, substituting (11) into (10), the plane-wave weights can be calculated as:

$$\gamma(n+1) = \gamma(n) - \mu_{\text{mic}} \mathbf{E}^H \mathbf{v}(n) - \frac{1}{2} \mu_{\text{mic}} \lambda_1 \left(\text{sgn}\{\Re\{\gamma(n)\}\} + i \text{sgn}\{\Im\{\gamma(n)\}\} \right). \quad (12)$$

3.2. Iteratively reweighted least squares (IRLS)

It is known that by introducing the ℓ_p -norm and solving the following optimization problem, where $0 < p < 1$ can provide a sparse solution with much fewer measurements than $p = 1$ [26], [27]:

$$\min_{\gamma} \|\gamma\|_p^p, \text{ s.t. } \mathbf{s} = \mathbf{E}\gamma. \quad (13)$$

Applying basis pursuit denoising (BPD) [28], (13) can be written in an unconstrained form as:

$$\min_{\gamma} \frac{1}{p} \|\gamma\|_p^p + \frac{\lambda_2}{2} \|\mathbf{v}\|_2^2. \quad (14)$$

Although the optimization problem (14) is a nonconvex function, we can adopt IRLS [27], [28] to solve it iteratively. IRLS is known to converge relatively fast in terms of the number of iterations, however, the algorithm includes matrix inversion in every iteration, which may lead to high computational cost. There is a fast implementation of the IRLS algorithm [29] to deal with this issue.

4. MODE-DOMAIN ACTIVE NOISE CONTROL

In this section, we describe a mode-domain adaptive filtering algorithm based on the filtered-x least mean square (FxLMS) algorithm [30]. Consider two circular microphone arrays placed in a free field, as depicted in Fig. 2. The outer circle is a reference microphone array capturing reference signals, and the inner circle is an error microphone array, measuring the residual signals. Between

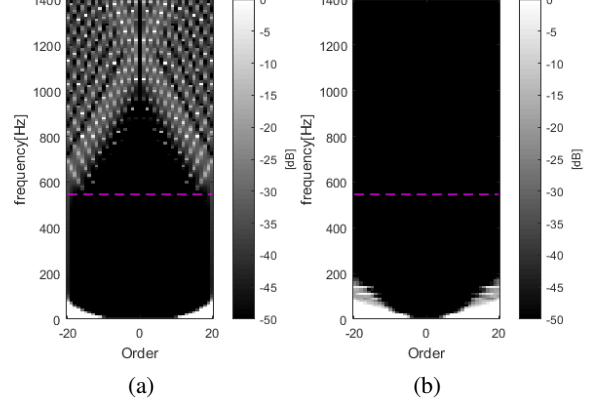


Fig. 4. Mode coefficients error between original and reconstructed noise field. The horizontal broken line indicates the spatial Nyquist frequency. (a) MDFF. (b) Proposed ($p = 0.5$).

those two microphone arrays, a circular loudspeaker array is placed to drive the anti-noise signals.

Adopting the mode-domain feedforward (MDFF) FxLMS algorithm, a residual mode coefficient at step n can be written as:

$$e_m(n, k) = \beta_m(k) + w_m(n, k) x'_m(n, k), \quad (15)$$

where $w_m(n, k)$ is the m th-order mode weight of the adaptive filter, $x'_m(n, k) = g_m(k) x_m(n, k)$ is the m th-order filtered reference mode coefficient, $g_m(k)$ is the m th-order mode coefficient of the acoustic transfer function of the loudspeaker, and $x_m(n, k)$ is the m th-order reference mode coefficient. In the 2D free-field space, $g_m(k) = -\frac{i}{4} H_m^{(2)}(kR_s)$, where $H_m^{(2)}(\cdot)$ is the second-kind Hankel function of order m , and R_s is the radius of the loudspeaker array. The reference mode coefficient can be calculated as

$$x_m(n, k) = i^m \sum_{\ell=1}^L \gamma_{\ell}(n, k) e^{-im\phi_{\ell}}, \quad (16)$$

using $\gamma_{\ell}(n, k)$ reconstructed from the reference signals by solving the optimization problem mentioned in the previous section. Finally, filtered-x normalized least mean square (FxNLMS) [31] algorithm updates the mode weight as:

$$w_m(n+1, k) = w_m(n, k) - \mu_{\text{sp}} \frac{e_m(n, k) \overline{x'_m(n, k)}}{x'_m(n, k) \overline{x'_m(n, k)}}, \quad (17)$$

where $\overline{(\cdot)}$ denotes the complex conjugate operation and μ_{sp} is the step size.

5. EXPERIMENT

We evaluated and compared the accuracy of the reconstructed reference mode coefficients and noise attenuation level among following methods: (i) MDFF corresponds to the conventional method based on (3) and (17) as a baseline; (ii) Proposed (L1) corresponding to the ℓ_1 -norm constrained ANC method based on (12); (iii) Proposed ($p = 1$); and (iv) Proposed ($p = 0.5$), corresponding to the IRLS method based on (14). Since reference microphones for ANC are typically placed outermost, the reference-mode coefficients are more likely to be affected by spatial aliasing artefacts. To overcome this problem, we applied the proposed method to the reference microphone array outputs.

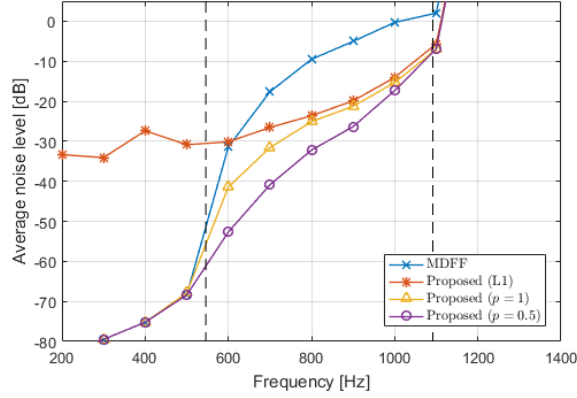


Fig. 5. Average noise level at several frequency bins after 50 iterations. The vertical broken lines indicate the spatial Nyquist frequencies corresponding to the reference (left) and the error (right) microphone array.

The radii of the error and reference microphone arrays are 1 m and 2 m, respectively. Each microphone array consists of 41 omni-directional microphones. The loudspeaker array consists of 41 monopole loudspeakers and the radius is 1.5 m. The maximum order of the mode coefficients is $M = 20$. For these experimental conditions, the spatial Nyquist frequency corresponding to the reference microphone array is 546 Hz, and to the error microphone array is 1092 Hz. We use $L = 128$ plane waves to construct the over-complete matrix \mathbf{E} .

5.1. Reference mode coefficient accuracy

We calculated the signal-to-distortion ratio (SDR) [32] inside the control region depicted as a colored region in Fig. 2 to measure the accuracy of the noise field reproduced from the reference signals, which is important to attenuate the noise field properly in feedforward ANC.

Figure 3 shows the frequency dependent SDR calculated using several methods. The circular expansion is based on (3). The SDRs using the proposed method were calculated after convergence. We can clearly see that above the spatial Nyquist frequency, the circular expansion method can no longer reproduce the noise field accurately, while the proposed methods can provide better accuracy at higher frequencies. Figure 4 depicts the mode coefficient error vs frequency and shows spatial aliasing artifacts. There are higher errors appearing from higher modes above the spatial Nyquist frequency in MDFF. Note that the higher errors in the evanescent region have only minimal impact on the ANC system, as previously mentioned.

Our preliminary experiment shows that the convergence speed vary among each method. For example, Proposed (L1) needs around 100 iterations to converge, whereas, Proposed ($p = 0.5$) needs only around 10 iterations.

5.2. Noise attenuation level

We performed adaptive ANC by adopting several methods and evaluating the noise attenuation level. Figure 5 shows the noise attenuation level at several frequencies after 50 iterations. The vertical broken lines indicate the spatial Nyquist frequencies correspond to the reference microphone array and the error microphone array, respec-

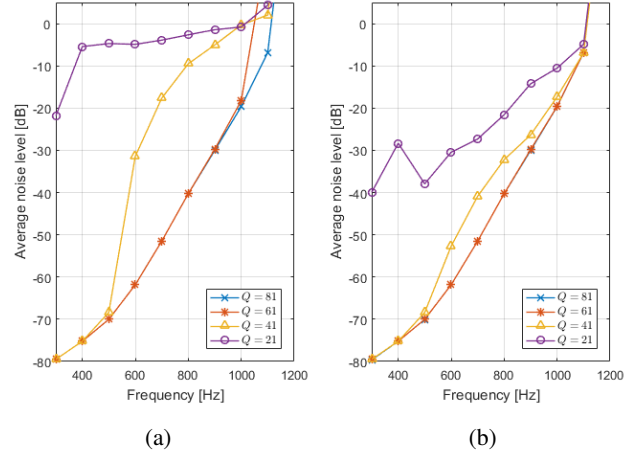


Fig. 6. Average noise level among various setups for the number of reference microphones. (a) MDFF. (b) Proposed ($p = 0.5$).

tively. Below the Nyquist frequency of the reference microphone array, the MDFF and the proposed method gave almost the same results except Proposed (L1), which gave even worse performance. We found that this was due to the strength of the constraint that was controlled by the parameter λ_1 . The ℓ_1 constraint was too strong to calculate accurate reference mode coefficients for lower frequencies below the spatial Nyquist frequency. We confirmed that the result improved once we manually tuned the parameter for each frequency, however, we use a fixed parameter in this paper since the issue is out of the scope and also we are not tuning any parameters for other methods.

For higher frequencies, the attenuation level of MDFF degrades due to spatial aliasing, however, the proposed method can still attenuate the noise. Above the Nyquist frequency of the error microphone array, all methods were out of control and no attenuation could be achieved.

5.3. Reduction of the number of reference microphones

When the noise field can be expressed by a sparse set of plane wave weights, we can reduce the number of reference microphones to calculate the reference mode coefficients. Figure 6 shows the average noise level after 50 iterations of ANC. Recalling the Nyquist frequency of the reference microphone array, it is natural that the noise attenuation performance starts degrading above 546 Hz for $Q = 41$ and 1092 Hz for $Q = 81$ in MDFF. On the other hand, we can see that the proposed method performs well over frequencies even though we reduced the number of reference microphones. For both methods, the ANC system starts diverging above 1092 Hz, which is the Nyquist frequency of the error microphone array.

6. CONCLUSION

In this paper, we explored the mode-domain feedforward ANC system performance using sparse signal representation for the reference signals. We compared several CS methods and showed that the IRLS algorithm with $p = 0.5$ performs well in terms of both convergence speed and noise attenuation level. We showed that the proposed method can attenuate the noise field beyond the spatial Nyquist frequency even with fewer reference microphones than required by spatial sampling theory.

7. REFERENCES

- [1] S. M. Kuo and D. R. Morgan, *Active noise control systems: algorithms and DSP implementations*, New York: Wiley, 1995.
- [2] S. M. Kuo and D. R. Morgan, "Active noise control: a tutorial review," *Proc. IEEE*, vol. 87, no. 6, pp. 943–973, Jun. 1999.
- [3] Y. Kajikawa, W.-S. Gan, and S. M. Kuo, "Recent advances on active noise control: open issues and innovative applications," *APSIPA Trans. Signal Inform. Process.*, vol. 1, pp. 1–21, 2012.
- [4] S. Elliott, I. Stothers, and P. Nelson, "A multiple error LMS algorithm and its application to the active control of sound and vibration," *IEEE Trans. Acoust., Speech, Signal Process.*, vol. 35, no. 10, pp. 1423–1434, Oct. 1987.
- [5] H. Chen, P. Samarasinghe, T. D. Abhayapala, and W. Zhang, "Spatial noise cancellation inside cars: Performance analysis and experimental results," in *Proc. IEEE Workshop on Applications of Signal Processing to Audio and Acoustics (WASPAA)*, 2015, pp. 1–5.
- [6] P. N. Samarasinghe, W. Zhang, and T. D. Abhayapala, "Recent advances in active noise control inside automobile cabins: Toward quieter cars," *IEEE Signal Process. Mag.*, vol. 33, no. 6, pp. 61–73, Nov. 2016.
- [7] S. C. Douglas, "Fast implementations of the filtered-X LMS and LMS algorithms for multichannel active noise control," *IEEE Speech Audio Process.*, vol. 7, no. 4, pp. 454–465, Jul. 1999.
- [8] M. Bouchard and S. Norcross, "Computational load reduction of fast convergence algorithms for multichannel active noise control," *Signal Process.*, vol. 83, no. 1, pp. 121–134, 2003.
- [9] A. J. Berkhout, D. de Vries, and P. Vogel, "Acoustic control by wave field synthesis," *J. Acoust. Soc. Amer.*, vol. 93, no. 5, pp. 2764–2778, 1993.
- [10] M. A. Poletti, "A unified theory of horizontal holographic sound systems," *J. Audio Eng. Soc.*, vol. 48, no. 12, pp. 1155–1182, 2000.
- [11] T. D. Abhayapala and D. B. Ward, "Theory and design of high order sound field microphones using spherical microphone array," in *Proc. ICASSP*, 2002, vol. 2, pp. 1949–1952.
- [12] D. R. Morgan, "An adaptive modal-based active control system," *J. Acoust. Soc. Amer.*, vol. 89, no. 1, pp. 248–256, Jan. 1991.
- [13] S. Spors and H. Buchner, "Efficient massive multichannel active noise control using wave-domain adaptive filtering," in *Proc. IEEE 3rd Int. Symp. Communications, Control and Signal Processing*, 2008, pp. 1480–1485.
- [14] J. Zhang, W. Zhang, and T. D. Abhayapala, "Noise cancellation over spatial regions using adaptive wave domain processing," in *Proc. IEEE Workshop on Applications of Signal Processing to Audio and Acoustics (WASPAA)*, 2015, pp. 1–5.
- [15] J. Ahrens, *Analytic Methods of Sound Field Synthesis*, New York: Springer, 2012.
- [16] E. J. Candès and M. B. Wakin, "An introduction to compressive sampling," *IEEE Signal Process. Mag.*, vol. 25, no. 2, pp. 21–30, Mar. 2008.
- [17] D. Malioutov, M. Cetin, and A. S. Willsky, "A sparse signal reconstruction perspective for source localization with sensor arrays," *IEEE Trans. Signal Process.*, vol. 53, no. 8, pp. 3010–3022, Aug. 2005.
- [18] N. Epain, C. Jin, and A. Van Schaik, "The application of compressive sampling to the analysis and synthesis of spatial sound fields," in *Proc. 127th Audio Engineering Society Convention*, Oct. 2009.
- [19] J. Zhang, T. D. Abhayapala, P. N. Samarasinghe, W. Zhang, and S. Jiang, "Sparse complex FxLMS for active noise cancellation over spatial regions," in *Proc. ICASSP*, 2016, pp. 524–528.
- [20] J. Zhang, T. D. Abhayapala, P. N. Samarasinghe, W. Zhang, and S. Jiang, "Multichannel active noise control for spatially sparse noise fields," *J. Acoust. Soc. Amer.*, vol. 140, no. 6, pp. EL510–EL516, 2016.
- [21] R. A. Kennedy, P. Sadeghi, T. D. Abhayapala, and H. M. Jones, "Intrinsic limits of dimensionality and richness in random multipath fields," *IEEE Trans. Signal Process.*, vol. 55, no. 6, pp. 2542–2556, Jun. 2007.
- [22] D. B. Ward and T. D. Abhayapala, "Reproduction of a plane-wave sound field using an array of loudspeakers," *IEEE Speech Audio Process.*, vol. 9, no. 6, pp. 697–707, Sep. 2001.
- [23] P. Samarasinghe, T. Abhayapala, and M. Poletti, "Wavefield analysis over large areas using distributed higher order microphones," *IEEE/ACM Trans. Audio, Speech, Language Process.*, vol. 22, no. 3, pp. 647–658, Mar. 2014.
- [24] E. G. Williams, *Fourier Acoustics: Sound Radiation and Nearfield Acoustical Holography*, New York: Academic press, 1999.
- [25] C. Fan, S. M. A. Salehin, and T. D. Abhayapala, "Practical implementation and analysis of spatial soundfield capture by higher order microphones," in *Proc. Asia-Pacific Signal and Information Processing Association Annual Summit and Conference (APSIPA ASC)*, 2014, pp. 1–8.
- [26] R. Chartrand, "Exact reconstruction of sparse signals via non-convex minimization," *IEEE Signal Process. Lett.*, vol. 14, no. 10, pp. 707–710, 2007.
- [27] R. Chartrand and W. Yin, "Iteratively reweighted algorithms for compressive sensing," in *Proc. ICASSP*, 2008, pp. 3869–3872.
- [28] R. E. Carrillo and K. E. Barner, "Iteratively re-weighted least squares for sparse signal reconstruction from noisy measurements," in *Proc. 43rd IEEE Annu. Conf. Inf. Sci. Syst. (CISS)*, 2009, pp. 448–453.
- [29] C. Chen, J. Huang, L. He, and H. Li, "Fast iteratively reweighted least squares algorithms for analysis-based sparsity reconstruction," *arXiv preprint arXiv:1411.5057*, 2014.
- [30] J. C. Burgess, "Active adaptive sound control in a duct: A computer simulation," *J. Acoust. Soc. Amer.*, vol. 70, no. 3, pp. 715–726, 1981.
- [31] D. T. M. Slock, "On the convergence behavior of the LMS and the normalized LMS algorithms," *IEEE Trans. Signal Process.*, vol. 41, no. 9, pp. 2811–2825, Sep. 1993.
- [32] S. Koyama, S. Shimauchi, and H. Ohmuro, "Sparse sound field representation in recording and reproduction for reducing spatial aliasing artifacts," in *Proc. ICASSP*, 2014, pp. 4443–4447.